

E-6-4

Low Voltage Actuated RF MEMS Switches Using Push-Pull Operation

Dooyoung Hah, Euisik Yoon and Songcheol Hong

Department of Electrical Engineering and Computer Science, KAIST, 373-1, Kusong-dong, Yusong-gu, Taejeon, Korea
 Phone: +82-42-869-8071, Fax: +82-42-869-8560, E-mail: hady@cais.kaist.ac.kr

1. Introduction

Microelectromechanical systems (MEMS) technology is expected to become a significant tool in the design of the radio-frequency (RF) communication systems. Especially, RF MEMS switches [1-2] have been paid great attention due to their excellent electrical performance compared to the semiconductor counterparts. However, their main drawback is the high actuation voltage (typically, >20V). In this work, we demonstrate the low voltage actuated RF MEMS switches with the push-pull configuration.

2. Push-Pull Configuration

Fig. 1 shows the schematic diagram of the RF MEMS switch. The isolation of the switch at the off state is determined by the off-capacitance (C_{off}). Because capacitance is inversely proportional to the distance between its two electrodes, the isolation becomes larger if the contact is lifted higher. For this purpose, we utilize a push-pull configuration. There are two fixed electrodes, a 'push' electrode and a 'pull' electrode, on the substrate. When voltage is applied to the pull electrode as Fig. 2(a), the contact moves down to make contact with the signal line. When this pull voltage is eliminated and the push voltage is applied as Fig. 2(b), the contact is lifted upward. The contact height (h_c) at the off state is amplified by the leverage, which is expressed as,

$$h_c = \left(2 + \frac{l_{lever}}{l_{re}} \right) h_0 \quad (1)$$

where, l_{lever} is the length of the lever, l_{re} is the half-length of the rotating electrode, and h_0 is the initial contact height. It shows that h_c , hence isolation, increases as l_{lever} increases. Therefore, we can make h_0 lower to reduce the actuation voltage while maintaining high isolation.

3. Design

Mechanical Consideration

The actuation voltage is determined by the geometrical dimensions and the material properties of the torsion springs and the rotating electrode. Gold is selected as the structure material due to its low shear modulus and low residual stress. Two types of springs are tested. One is the straight-type spring (Fig. 3(a), $20\mu\text{m}$ (w) \times $300\mu\text{m}$ (l) \times $1.4\mu\text{m}$ (t)) and the other is the serpentine-type spring (Fig. 3(b), $20\mu\text{m}$ (w) \times $900\mu\text{m}$ (l) \times $1.4\mu\text{m}$ (t)). l_{re} varies from $100\mu\text{m}$ to $400\mu\text{m}$. The switch actuated by both torsion and bending is also attempted (Fig. 4). The bending electrode is added to this type of switch.

RF Consideration

The contact area has to be designed carefully to have good RF performance. As the contact area increases, on-resistance (R_{on}) decreases and C_{off} increases. The designed contact area is $90 \times 90\mu\text{m}^2$. The signal line gap is $20\mu\text{m}$. The SPDT (single-pole double-throw) switch (Fig. 5) is also

designed, which is inherently made by the push-pull configuration.

4. Fabrication

Semi-insulating GaAs has been used as the substrate. At first, the signal line and the fixed (push and pull) electrodes are formed by gold plating. AZ5214 photoresist is spun as a sacrificial layer and anchors are defined. The contact is formed by gold plating. The movable structure is formed as a multi-layer of SiN_x ($0.2\mu\text{m}$) - titanium/gold ($20/50\text{nm}$) - plated gold ($1.1\mu\text{m}$) as a stress compensated structure. Finally, the structure is released by O_2 plasma dry etching.

5. Experiment Results

The C-V measurement result of the fabricated switch is depicted in Fig. 6. The capacitance changes abruptly at the threshold voltage. Measured on-voltage (V_{pull}) and off-voltage (V_{push}) are summarized in Table I. It shows that the actuation voltage decreases as l_{re} increases and is not varied much by the spring length (l_s). It also shows that the actuation voltage of the switch with serpentine-type springs is lower than that with straight-type springs. The minimum actuation voltage is measured as 5V. In the combined actuation switch, V_{pull} is measured as 10.7V with torsional actuation only and as 11.9V with bending actuation only. It becomes 7.2V by the combination of torsional and bending actuation. The closure time of the switch is measured as 0.6ms. The RF characteristics from 500MHz to 4GHz of the fabricated switch are examined with HP8720C network analyzer (Fig. 7). The insertion loss is below 2dB up to 4GHz. This relatively large insertion loss may be due to the parasitic capacitance between the contact part and the rotating electrode. At zero bias, the isolation is measured as >17dB. It becomes >28dB in the 'push' operation, improving the isolation by ~10dB. The isolation will be improved more with the wider signal line gap. R_{on} is measured as 10Ω . C_{off} is 70fF at zero bias and reduced to 15fF at the off state.

6. Conclusions

Surface-micromachined microwave switches with push-pull configuration have been demonstrated. The actuation voltage as low as 5V has been achieved by means of torsion springs and leverage. RF characterizations show that the isolation can be significantly improved by the push-pull configuration. These switches can be used for mobile RF telecommunication systems.

Acknowledgements

This work is partially supported by the National Research Laboratory project and The Millimeter-wave Innovation Technology research center. The authors would like to thank D. Baek, M. Kim, E. Park, and Y. Kang for their fabrication aid.

References

- [1] J. J. Yao and M. F. Chang, *Proc. 8th Int. Conf. Solid-State Sens. Actuators and Eurosensors IX* (1995) p. 384.
 [2] C. Goldsmith, Z. Yao, S. Eshelman, and D. Denniston, *IEEE Microwave and Guided Wave Letters*, **8**, 269 (1998).

Table I The measured actuation voltages of the switches.

spring type	l_s [μm]	l_{re} [μm]	l_{lever} [μm]	V_{pull} [V]	V_{push} [V]
straight	300	100	200	10	16
straight	300	200	400	4	6
straight	300	400	800	2	5
straight	100	200	400	4	6
straight	500	200	400	4	7
serpentine	900	200	400	4	6
serpentine	1140	200	400	2	5

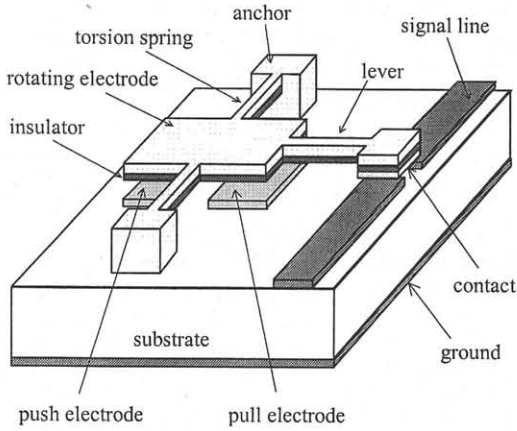


Fig. 1 The schematic diagram of the proposed switch.

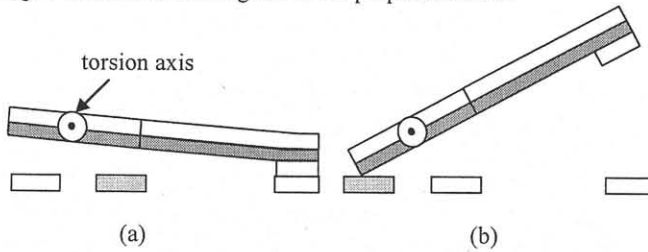


Fig. 2 The switch at (a) the on state and (b) the off state.

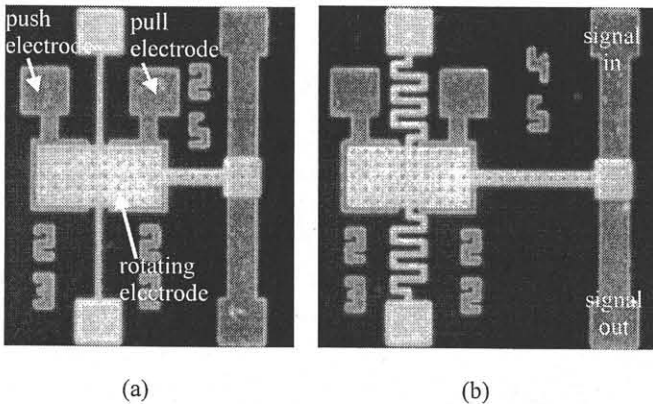


Fig. 3 The micrograph of the switches with (a) straight-type springs and (b) serpentine-type springs.

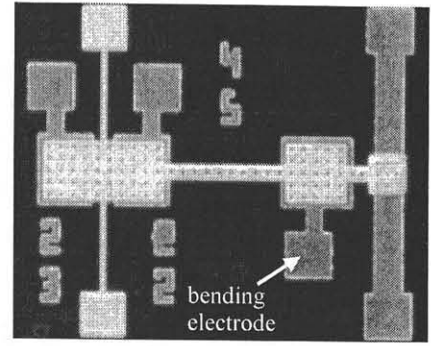


Fig. 4 The micrograph of the switch with the combined actuation.

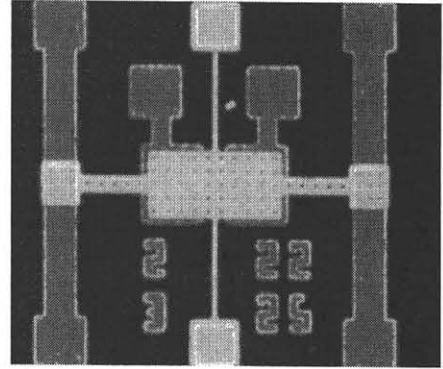


Fig. 5 The micrograph of the SPDT switch.

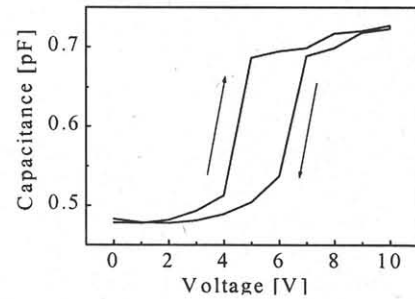


Fig. 6 The C-V measurement result of the switch.

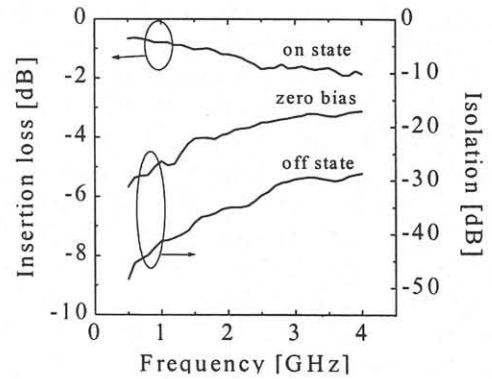


Fig. 7. The RF characteristics of the switch.